Turbidity Level Prediction Based on Suspended Particle Counting Through Image Processing Approach

Temmy Wikaningrum[1], M. Galang Alvasa[2], Yandes Panelin[3], Rijal Hakiki[4*]

[1,2,3,4]Environmental Engineering Department, President University, Cikarang
***Correspondent email**: rijalhakiki@president.ac.id

Abstract
Monitoring of pollutant concentrations in surface water becomes a concern, considering the utilization of surface water as the raw water for drinking water treatment plants (WTP). The fluctuation of pollutant concentrations in surface water can affect the performance of WTP. This research was conducted to assess the potential for turbidity level prediction based on the calculation of the number and surface area of suspended particles through a digital image processing approach. Measurements of the amount and surface area were carried out in the form of laboratory-scale experiments using the open source software ImageJ 1.46r. The algorithm in ImageJ can convert pixels into a number "value" and surface area through a series of digital image processing steps, henceforth compared with the existing measurement method. The results showed that there was a strong correlation between the number of particles and the concentration of formazine suspension (r = 0.9821), but does not apply to the surface area. Referring to the results of laboratory experiments, it can be concluded that the approach to measure the number of suspended particles can be the basis for predicting the turbidity level in the turbidity range 100-800 NTU, but does not apply to the turbidity range 0.02-20 NTU.
Keywords: *suspended particles, water quality, surface water, raw water, turbidity level*

Abstrak
Pemantauan tingkat kekeruhan pada air permukaan menjadi perhatian sehubungan dengan pemanfaatan air permukaan sebagai sumber air baku instalasi pengolahan air minum (IPAM). Selain itu, fluktuasi tingkat kekeruhan telah diketahui dapat mempengaruhi kinerja IPAM. Penelitian ini dilakukan untuk mengkaji potensi prediksi tingkat kekeruhan berbasis penghitungan jumlah dan luas permukaan partikel tersuspensi dengan pendekatan pengolahan citra digital. Pengukuran jumlah dan luas permukaan dilakukan dalam bentuk percobaan skala laboratorium dengan bantuan perangkat lunak *open source* ImageJ 1.46r. Algoritma pada ImageJ dapat mengkonversi pixel menjadi "nilai" jumlah dan luas permukaan melalui serangkaian tahap pengolahan citra, untuk selanjutnya dibandingkan dengan metode pengukuran eksisting. Hasil penelitian menunjukkan bahwa terdapat korelasi yang cukup kuat antara jumlah partikel dengan konsentrasi suspensi formazin (r = 0.9821). Tetapi hal ini tidak berlaku pada luas permukaan partikel. Mengacu pada kajian terhadap hasil percobaan laboratorium, dapat disimpulkan bahwa pendekatan pengukuran jumlah partikel tersuspensi dapat menjadi dasar prediksi tingkat kekeruhan pada rentang kekeruhan 100-800 NTU, tetapi tidak berlaku pada rentang kekeruhan 0.02-20 NTU.
Kata Kunci: *air baku, air permukaan, partikel tersuspensi, kualitas air, tingkat kekeruhan*

1. Introduction

Fluctuations of pollutant concentrations in surface water may affect water treatment plants (WTP) performance. From the various water quality indicators, generally, turbidity is the parameter that being the indicators for WTP performance. In additions, this parameter becomes the reference for the chemical (coagulant) dosage in a treatment plants [1], [2]. Turbidity level also can be related to the bacteriological contamination of surface water, because in general, it tend to be suspended in water [3], [4]. In another words, we can say that bacteria is the one of turbidity component besides silica and other suspended materials.

At the existing turbidity level measurement, nephelometric method, the principle is based on the measurements of scattered light by photodetector at certain angle of detections and light source [5]. In these conditions, there are possibilities of disturbance caused by the light absorptions, false positive of the measurements caused by the interference of fluorescence effects from other pollutants (besides the suspended particles in a water sample). Bubbles and true water color are the examples of disturbance that

can affect the turbidity measurement level [5]. Referring to the phenomena, this article tried to identify the potential of turbidity measurements through suspended particle analysis by a preliminary laboratory trial for turbidity. The analysis include the process of particle counting and surface area measurements of suspended particle through image processing approach. While the existing turbidity measurement method based on the measurements of light intensity scattered by the suspended particle in the water sample.

According to the theory, there are several possible phenomena when a beam of light passes through the medium. Theoretically, it can be absorbed, refracted, reflected or diffracted by the medium [6]. Another literature state that nephelometric measurement method based on the optical-physics properties of materials (solutions). This optical properties includes the ability of the materials (solutions) to absorb the radiant energy (absorption), the ability to emit the radiation when it excited by an energy source (emission), or its ability to spread out the radiations (dispersion or scattering) [7].

The instruments to measure turbidity level usually consisted of the light source and one or more photoelectric detectors that can capture scattered light at the angel of 90° [8]. Referring to the standard method 2310B, there are several design criteria for turbidity level measurement instrument. The light source used was a tungsten-filament lamp that operate at color temperature between 2200-3000K, the distance that passed by the beam of light and the scattered light in a sample cell should be not more than 10 cm, the angel of the light captured by the detector should be not more than $90^o \pm 30^o$, and the last things is if it utilize the filter system on its detector, it should have spectral peak response between 400 and 600 nm [5].

Prior research articles have been written by the previous researchers, related to the topics of the determinations of turbidity levels. From the developments and improvements of the measurement method based on electronic sensor to the developments of turbidity level determinations involving the computational approaches through the image processing techniques. Previous researchers have tried to improve the performance of the turbidity measurement instrument by combining with the photodetector / photodiode (the detector) with several types of light sources such as infrared light emitting diode (LED) and utilization of GRINephy in a light source and the photodetector [9], [10].

2. Material and Methods

This research divided to 5 major steps including preparation, data acquisition, data process, data analysis, and synthesizing the conclusions. It includes several activities for each steps to assess the potential for turbidity level prediction based on the enumeration of the number and surface area of suspended particles through a digital image processing approach.

Preparation step

The 3D model design of measurement-chamber generated by the open source 3D modeling software FreeCAD 0.17. The design divided to several parts those are the main-chamber, camera holder, slide-chamber cover, and sample-cell holder as shown in **Fig. 1 (a)-(d)**. Main-chamber dimension are 140 mm in length, 80 mm in width and 70 mm in height. The main-chamber is the main part which other parts will attach to it. The camera holder parts dimension are 30.9 mm in width, 4 mm thickness, 15.45 mm in diameter for the half round shape and the height fitted to the main-chamber part. The dimension of slide-chamber cover is 140 mm in length and 80 mm in width, fitted to the main-chamber. While for the sample cell holder fitted to the shape and size of Eutech turbidimeter ECTN100IR sample cell.

The model then printed on Creality 3D Printer CR-10 Mini which took almost 12 hours to finish the printing process. The process and the results of the printing activities were presented on **Fig. 1 (e)-(g)**. The material used to build this chamber is polylactid acid (PLA) filament with 210^oC nozzle temperature and 60^oC bed temperature. Other activities were configuring the position of light sources and the 2 mega pixels macro USB camera.
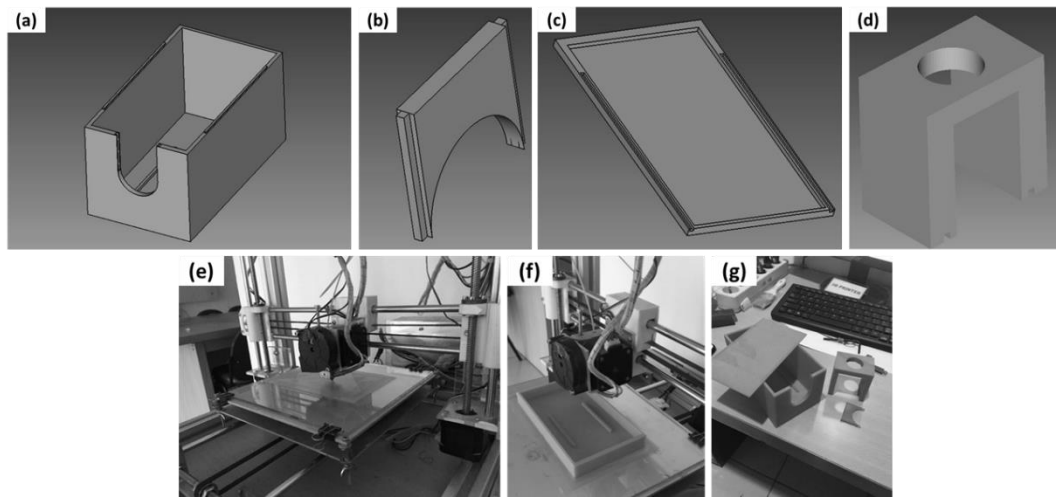
Fig. 1. 3D model of measurement chamber design (a) main-chamber; (b) camera holder;
(c) slide-chamber cover; (d) sample-cell holder; (e)-(f) The printing process;
and (g) the printing results of the 3D model design
Source: Author's documentation (2020)

Data Acqusition, Data Process and Data Analysis

The commercial Eutech turbidimeter ECTN100IR calibrated with the formazine standard series with various concentrations of 0.02, 20, 100, and 800 NTU following the calibrations manual of its instrument. The formazine standard then measured by the calibrated turbidimeter and video captured by the measurement-chamber prototype which produced from the previous preparation step. The captured video then extracted to thirty sequential images for a second interval for each image. Image acquisition process provided on **Fig. 2 (a)**, while the image processing steps were presented on **Fig. 2 (b)** and **Fig. 2 (c)**.

The acquired images then processed by the open source software ImageJ 1.46r through several steps of treatment. The one of principle in image processing deal with the separation of background and the foreground from the image [11]. Water surface as the background of the image while the suspended particles as the foreground that will be counted from the image. Generally, this separation process involves the thresholding and segmentation process to get the clear suspended particles separated image [12].
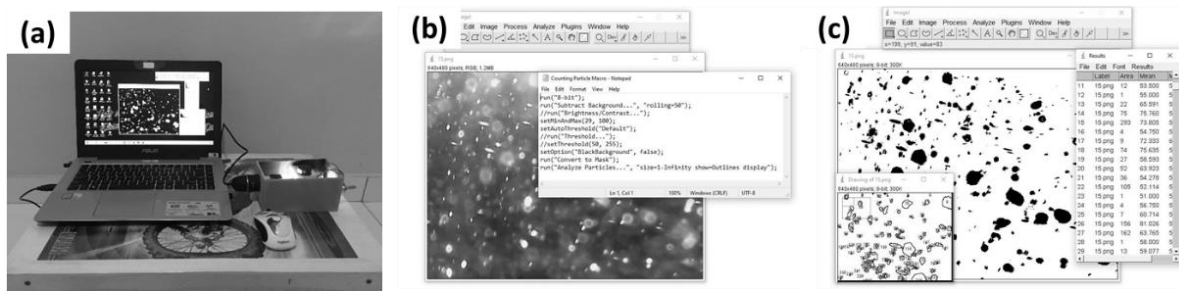
Fig. 2. Data acquisition step (a) and data processing with ImageJ 1.46r (b), (c)
Source: Author's documentation (2020)

This processing method formerly used for bacterial cell/colony counting both automatically or manually, such already conducted by several previous researchers. Ref. [2] has been conducted the automated colony and cell counting by digital image analysis based on edge detection [13]. The counting method involve the use of ImageJ macro which valuable in counting cells/colonies, measuring the area, volume, morphology and intensity [14]. In line to ref. [15]which is compare two automatic cell-counting solutions for fluorescent microscopic image. It shown that there was high correlation between automatic and manual counting method. Ref. [16] has conducted a research based on the ImageJ toolbox features to count the mammalian cells automatically in a hemocytometer assembled to the conventional light microscope with a webcam. It shown that this approach about ten times faster and more consistently

reliable compared to the manual counting. Referring to these previous researches, it can be seen that there are possibilities to apply this method as the approach for turbidity level measurements.

The resulted data from ImageJ software can be in a form of detail one-by-one counting data, or in a form of average data [17]. To answer the objectives of this research we used the detail output text data which will further process to find out the trends and use the correlation and regression test between the commercial turbidity with image processing based turbidity measurements. The overall description of the research stages is presented in **Fig. 3**.
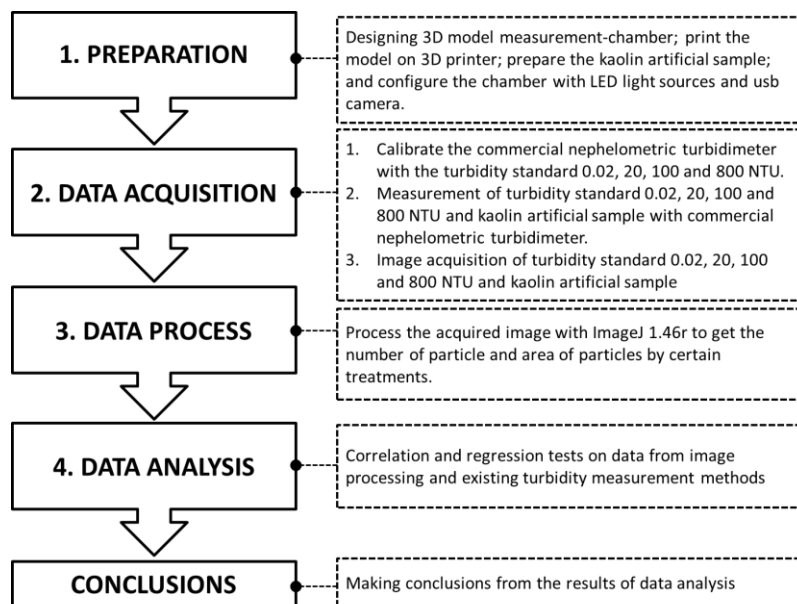
Fig. 3. The study of turbidity measurement through particle counting and surface
area measurements of suspended particle with image processing approach
Source: Author's documentation (2020)

3. Results and Discussion
Measurement-Chamber Configurations

Basically, the chamber configurations follow the design criteria Referring to the standard method 2310B with several modifications suit to this research. The chamber built with the purpose to inhibit ambient light interference that will affect the measurement results. The configurations and its modifications is provided in **Table 1**.

Table 1. Measurement-chamber configurations

Parameter	Design Criteria [5][*] (Standard Method 2310B)	Configured Measurement Chamber[**]
Light source	Tungsten-filament lamp (color temperature between 2200 and 3000°K)	Light emitting diode (LED) lamp (95 lux intensity)
Distance traversed by incident light and scattered light within the sample tube	< 10 cm	2 cm (camera to sample cell distance)
Angle of light acceptance by detector	$90^o \pm 30^o$	90°
Spectral peak of detector / filter	400-600 nm	n/a
Detector	Photoelectric detector	2 MP usb macro camera + ImageJ 1.46r

Source: [*] APHA (1999); [**] Author's documentation (2020)

Refer to the laboratory experiment results, several factors can affect measurement results such as ambient light interference, light source intensity, the distance between camera and sample cell, the angel of light source, the angel of camera, as well as dark background implementation [18]. In measuring turbidity with the enumeration approach of suspended particles, the number of particles and the calculated surface area are then substituted into the linear equation as a result of the measurement of the number of particles and the measurement results with a commercial turbidimeter against the standard series of

formazine suspensions. In this case the ambient light interference can produce a measurement bias due to the measured reflection of ambient light by the sample cell when it is quantified with ImageJ. This can happen because the foreground and background subtraction process is based on the difference between the dark and the light region in the analyzed image. Likewise with the light source intensity, lighting angle and dark background that were applied in the image acquisition stage, were also greatly affect the foreground and background subtraction process [11]. Meanwhile, the distance between the camera and the sample cell, as well as the shooting angle, will affect the camera's focus in producing images with the appropriate clarity and can be further processed with ImageJ. The difference in the results of the captured image at two different light intensity conditions is presented in **Fig. 4**.
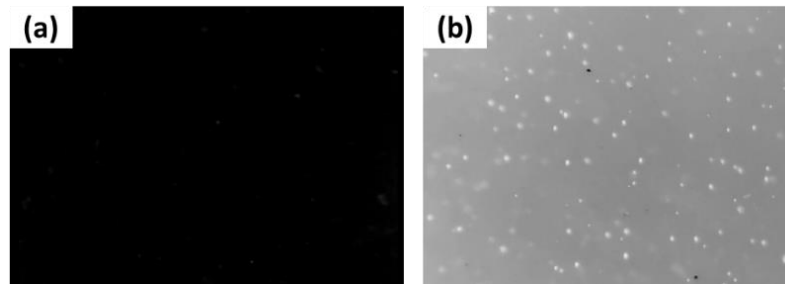
Fig. 4. The captured image in different light intensity
conditions (a) 65 lux and (b) 95 lux
Source : Author's documentation (2020)

On **Fig. 4.** it can be observed that the difference in light intensity applied will affect the image captured by the camera. In application conditions, the measured light source intensity is 65 lux, only black is visible in the image. Whereas in the application conditions the measured light source intensity is 95 lux, it can be seen that the white point of the suspended particles can be distinguished from the background. It can be assumed that the measurement-chamber configuration, control and adjustments to various influencing factors are carried out to produce sufficient contrast to produce an image which can then be subtracted and enumerated the number of suspended particles. Another factor that was not examined in this study was the factor that influenced the true color of the sample solution. This needs to be studied further because it has the potential to affect the contrast between the background and foreground.

In practice, the intensity of the light source is generated by adjusting the current in the LED lamp through a potentiometer while observing the video output captured by the camera. When it is observed that sufficient contrast is obtained as shown in **Fig. 4** (b), then measured the light intensity with a digital lux meter to determine the value of the light intensity that was applied in the measurement. The 95 lux value is a reference for each measurement treatment in this study. It is important to ensure that all factors that can affect measurements are made in a constant state. This is done to avoid/reduce the bias of the measurement results due to the effect of changing these factors. Or it can be said that the factors that are thought to influence the measurement results are used as control variables whose values are fixed

Digital Image Processing Results

Measurement of the level of turbidity based on enumeration of suspended particles involves the use of software in terms of its quantification. This is different from the existing turbidimeter measurement method which uses a photoelectric sensor to quantify the turbidity level [19]. However, until now the measurement method using a photoelectric sensor (nephelometry) is still the standard method of measuring turbidity [5]. Therefore, in the implementation, the results of the enumeration of suspended particles were compared with the turbidity measurement results of the existing method to determine the correlation between the two treatments.

To ensure that the image processing stage uses the same parameter values for each digital image analyzed, command, and parameter values are arranged in the form of macro scripts as can be seen in **Fig. 2** (b). The quantification stage includes the image conversion process from rgb to 8-bit format, brightness/contrast settings with a minimum value of 29 and a maximum of 100, setting the threshold value (50, 255) to separate suspended particles from the background, and call a command "Analyze Particle" which is one of the functions contained in ImageJ. In **Fig.2** (c), it can be observed the difference in the original image produced by the camera, as well as an image of the subtraction of suspended particles from the background. In addition, it can also be observed the tabulation of data on the

quantification of the particle number, as well as the surface area of suspended particles measured from the results of the analysis of the digital image captured by the camera.

As previously stated, the enumeration of suspended particles includes the calculation of the number of particles as well as the measurement of the average area and the total area of suspended particles for 120 samples of digital images captured by the camera. This sample consisted of 30 digital images for each standard formazine suspension concentration of 0.02, 20, 100, and 800 NTU following Eutech ECTN100IR commercial turbidimeter calibration standard concentrations. The data resulting from digital image processing with ImageJ is in the form of listing data in csv format [20], which is then plotted the formazine standard concentration against the counted number of suspended particles. In addition, a standard formazine concentration plot was also carried out on the mean surface area and the measured total surface area of suspended particles. As presented in **Fig**. **5.**, **Fig. 6.**, and **Fig. 7**.
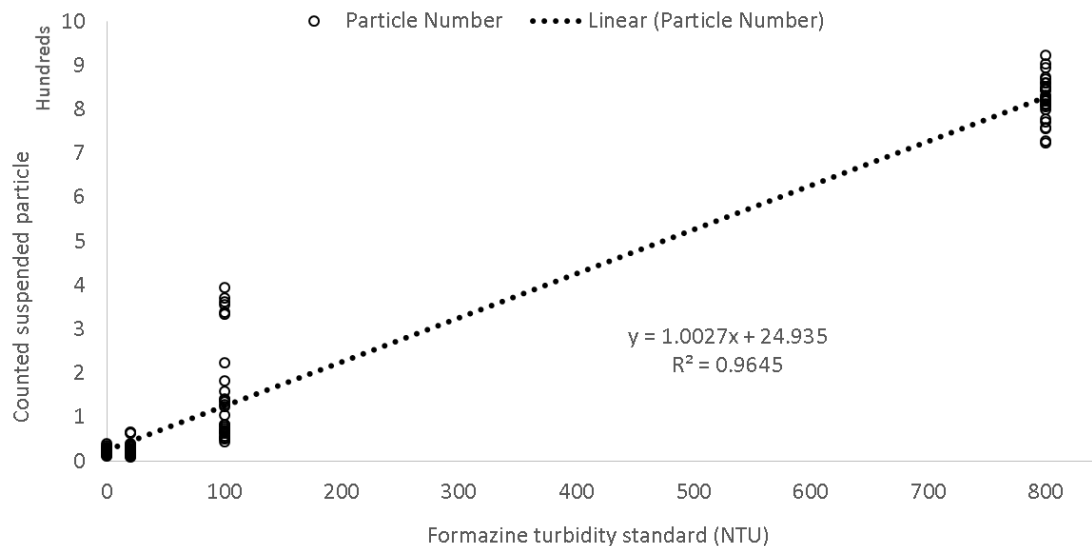
Fig. 5. The distribution pattern of the calculated number of particles for each
concentration of standard formazine suspension
Source: Data processing by the author (2020)

On **Fig. 5** can be observed the distribution pattern of the counting results of the number of suspended particles from 30 samples processed and analyzed by ImageJ. It can be observed that from a total of 120 samples consisting of 30 samples for each concentration, the values varied quite widely. This can be caused by the random movement of suspended particles in the water sample [21]. In this case, it is possible for the same particle to be counted more than once at different positions. However, the same calculation method is applied to each digital image captured by the camera for the four formazine suspension standards. The same treatment and method can reduce the resulting bias in measurement results. When observed further, the results of the calculation of the standard deviation for each concentration were 6.43 (0.02 NTU), 15.36 (20 NTU), 115.54 (100 NTU) and 47.43 (800 NTU), respectively.

This value showed that the results of the enumerated number of particles for each digital image at each concentration are not uniform. This is the basis for selecting measurements of 30 sample images captured by the camera. Because if the measurements only made for one image, the enumeration results cannot represent the number of particles contained in the sample. The distribution pattern of the measurement results for the mean area and the total area of the suspended particles for each sample at each concentration are presented in **Fig. 6**. and **Fig. 7**. The plots of the formazine standard concentration on the mean and total area of suspended particles showed quite varied results. This can be observed from the visualization of the results of the data plots and the results of the calculation of the standard deviation of the area, respectively 10.79 (0.02 NTU), 17.80 (20 NTU), 261.29 (100 NTU), 0.24 (800 NTU) for the results of measuring the mean area. Whereas for the measurement results of the total area of the particles, the calculated standard deviation were 333.17 (0.02 NTU), 851.86 (20 NTU), 97459.31 (100 NTU) and 300.15 (800 NTU), respectively.
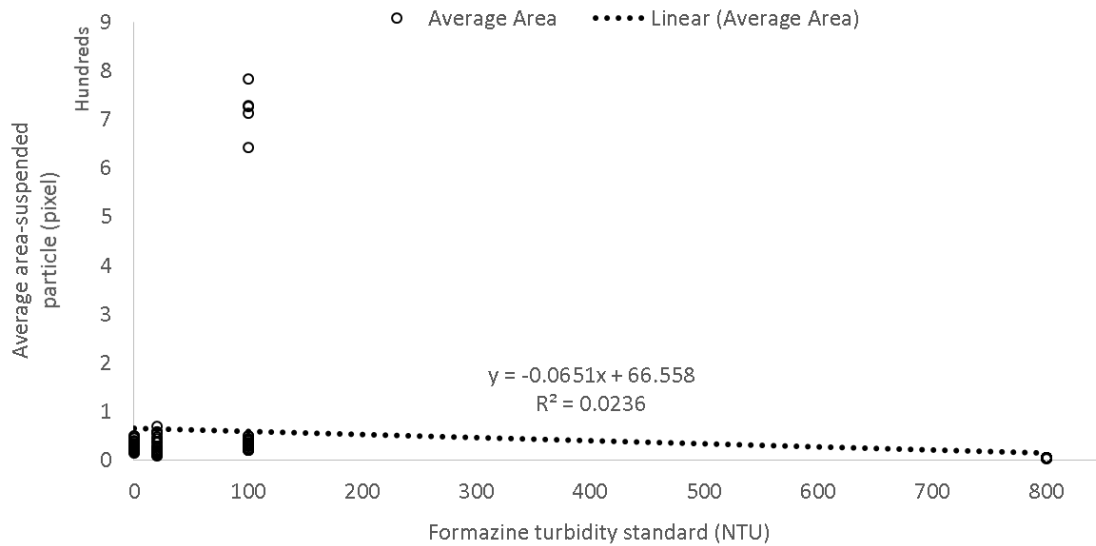
Fig. 6. The distribution pattern of the measurement results of the mean particle area for
each concentration standard formazine suspension
Source: Data processing by the author (2020)

The regression coefficient (R) which is the root of the coefficient of determination (R^2) in **Fig. 5**, **Fig. 6**, and **Fig. 7** are 0.9821, 0.1536 and 0.0064, respectively. This value shows the dependence of the dependent variable on the independent variable. The regression coefficient for the standard formazine VS counted particle concentration with a value close to 1 shows a dependence between the two variables. While the regression coefficient for the formazine standard concentration VS the area for mean and total shows a value close to 0, so it can be said that there is no dependence between variables. The results of the correlation test also show the same thing, as can be seen in **Table 2**. The correlation coefficient (r) of the formazine standard concentration to the counted particle, the mean area and total area were 0.9821, -0.1535, and -0.0637, respectively. This value shows the strength or weakness of the relationship between variables, which in this case can be observed that there is a very strong correlation between the standard formazine concentration and the counted particle. Meanwhile, the standard concentration of formazine on the area showed no correlation between variables for both mean and total area.
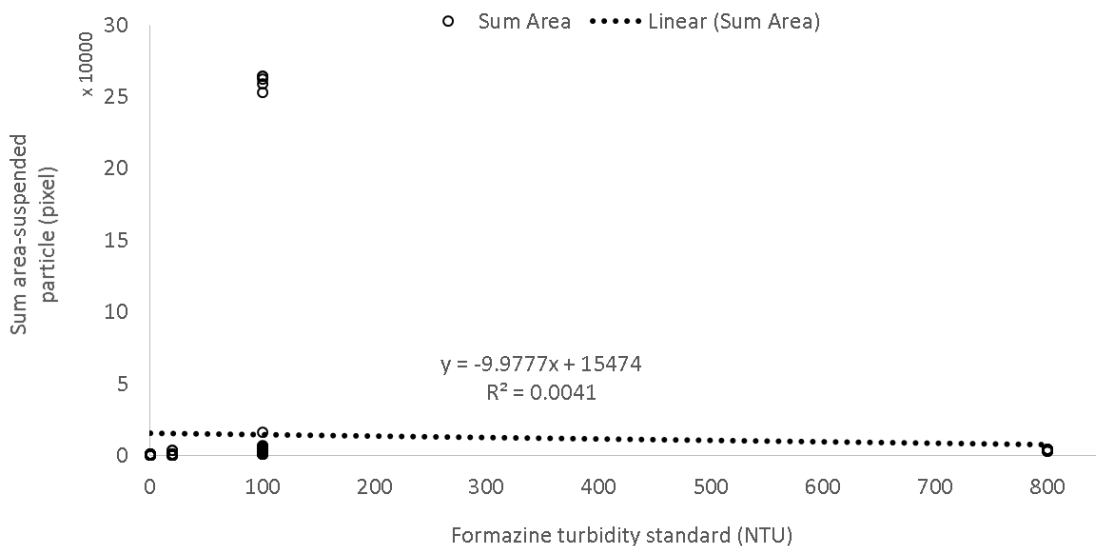
Fig. 7. The distribution pattern of the measurement results for the total particle area
for each concentration standard formazine suspension
Source: Data processing by the author (2020)

Based on the regression coefficient value obtained, henceforth, data processing will only be based on the particle count approach. In addition to visualizing the distribution pattern, the coefficient of determination and the value of the regression coefficient, other information that can be obtained is a simple linear regression equation. This equation is then used to predict the level of turbidity based on the

particle values measured at the digital image processing stage. Turbidity level prediction is done by substituting the counted particle value (y) to find out the turbidity value (x) in NTU units from the simple linear regression equation $y = 1.0027x + 24.935$.

Table 2. Correlation test on the results of data processing

	Formazine Standard (NTU)	Counted Particle	Average Area	Total Area
Formazine standard (NTU)	1.0000			
Counted particle	0.9821	1.0000		
Average area	-0.1535	-0.0046	1.0000	
Total area	-0.0637	0.0876	0.9924	1.0000

Source: Data processing by the author (2020)

Nephelometric Turbidimeter VS Suspended Particle Enumeration Approach

Another phenomenon that can also be observed from the results of laboratory experiments is in the same measurement conditions and measurement-chamber configuration, different measurement results can be obtained if there is a difference in the mean area of the suspended particles. This factor also explains that the mean and area of suspended particles do not have a strong correlation with the standard formazine concentration. As can be observed the results of the digital image capture in **Fig. 8** (a) is a 100 NTU formazine suspension with an average area of 29 pixels and a total particle area of 4077 pixels out of a total of 140 counted particles. Whereas in **Fig. 9** (b) is the kaolin suspension with a mean area of 64 pixels and a total particle area of 17121 pixels from a total of 267 particles counted. The constituent components of the suspension in the water sample can have various sizes [7]. Therefore, the determination of the turbidity level based on the mean value of the area or the total area of the particles cannot be used as an approach based on the results of observations in the laboratory.
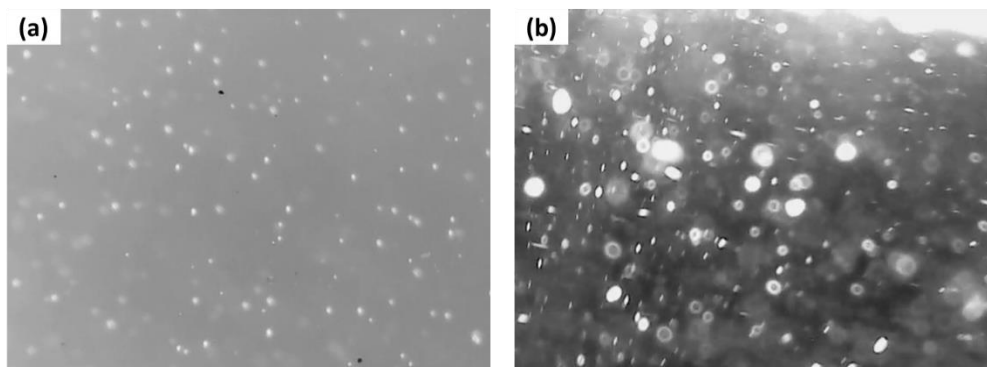
Fig. 8. Digital image captured by the camera (a) formazine 100 NTU suspension; (b) kaolin suspension
Source: Author's documentation (2020)

The suspended particle size expressed in mean area and total area does not correlate with the number of particles counted. Likewise with the standard concentration of formazine suspension which does not correlate with particle size, but correlates with counted particles. Based on this phenomenon, the approach to counting the number of particles is the chosen approach to determine the turbidity level in the water sample. To simplify the calculation, the substituted counted particle value is made in the form of the mean value from the measurement results of 30 digital image samples. A plot of the formazine standard concentrations against the mean counted particle is presented in **Fig. 9**. To find out the turbidity value, it can be calculated by the equation $x = (y - 24{,}935) / 1.0027$
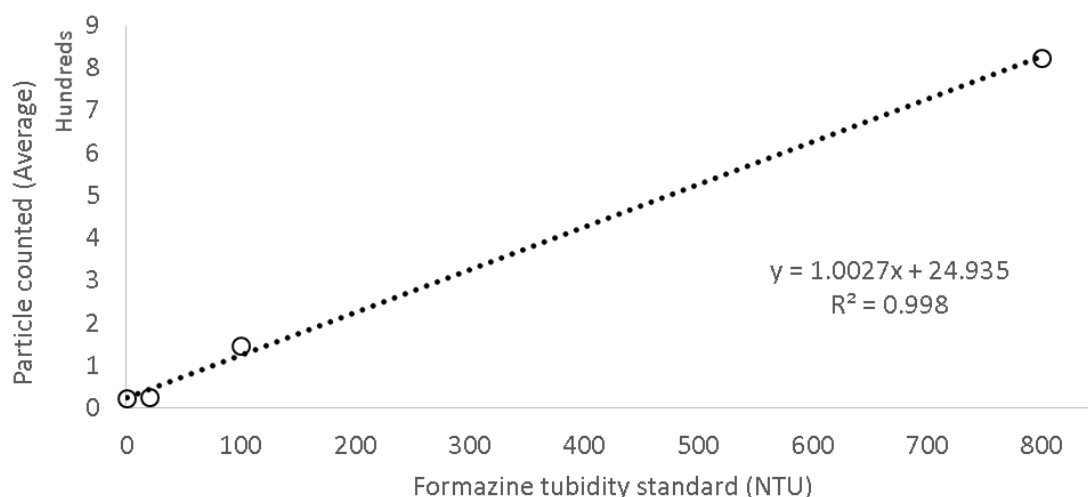
Fig. 9. Plot of formazine suspension standard series against the calculated particle mean
Source: Data processing by the author (2020)

Table 3 shows the results of the turbidity concentration prediction compared with the measurement results of the Eutech ECTN100IR commercial turbidimeter. Although the results of the correlation and regression tests show a relationship and dependence between the two variables, the calculation results do not show the same thing. The prediction of the level of turbidity using the particle count approach has not been able to show a value that is close to the measurement results of the Eutech ECTN100IR commercial turbidimeter. It can be observed that the prediction value, the measurement value of Eutech ECTN100IR and the calculated value of the standard formazine suspension of 0.02 NTU are 0.02, 0.02 and -1.93, respectively. In the standard measurement of 20 NTU formazine suspension, the predicted values, the Eutech ECTN100IR measurement values and the calculated values were 20.00, 19.99, and 1.36, respectively. In the standard measurement of formazine suspension 100 NTU, the predictive value was obtained, the Eutech ECTN100IR measurement value and the calculated value were 100.00, 100.00, and 123.00, respectively. In the standard measurement of formazine 800 NTU suspension, the predicted values were obtained, the Eutech ECTN100IR measurement values and the calculated values were 800.00, 797.00, and 797.61, respectively.

Table 3. Turbidity level prediction results in various samples

Sample	Predicted Concentration (NTU)	Eutech ECTN100IR Measurement Results	Particle Counted (Average)	Calculated NTU
Formazine 0.02 NTU	0.02	0.02	23.00	-1.93
Formazine 20 NTU	20.00	19.99	26.30	1.36
Formazine 100 NTU	100.00	100.00	148.27	123.00
Formazine 800 NTU	800.00	797.00	824.70	797.61
Kaolin sample	Unknown	253.48	267.00	241.41

Source: Data Processing by the Author (2020)

Meanwhile, on the turbidity measurements of kaolin suspension, the Eutech ECTN100IR measurement value was obtained and the calculated values were 253.48 and 241.41, respectively. These results indicate that at low turbidity levels (0.02 and 20 NTU) the predicted results are very far from predicted concentration. Meanwhile, at higher turbidity levels (100 and 800 NTU) the predicted results are relatively close to predicted concentration. This can be caused by various factors, including the effect of the resolution of the camera used, the effect of the threshold value, and the effect of the number of formazine standard suspension series measured in the experiment. The resolution of the camera used can affect the clarity of the processed digital image [22]. The sharper the resolution and the higher the level of focus of the camera, the clearer the difference between the background and the foreground will be [23]. This can improve the segmentation ability of suspended particles in the image, which means that it can affect the accuracy of the prediction results.

4. Conclusion

The results of laboratory experimental data processing indicate that the approach to measuring the number of suspended particles can be the basis for predicting turbidity levels, based on the results of the correlation test which resulted in a correlation coefficient of 0.9821. Whereas in the particle surface area measurement approach, the correlation coefficient value is -0.1535 for the mean surface area and -0.0637 for the total surface area. So it cannot be used as a basis for predicting turbidity levels. Although based on the results of the correlation test with the particle number approach the correlation coefficient is close to 1, not all turbidity ranges produce predicted values that are close to those of commercial turbidimeters. The prediction results in the turbidity range 100-800 NTU show a value close to the measurement results of the Eutech ECTN100IR commercial turbidimeter. However, in the turbidity range 0.02-20 NTU, the prediction results show that the value cannot yet be close to the measurement results of the Eutech ECTN100IR commercial turbidimeter. Further efforts need to be made to improve the accuracy of the prediction results, and it is also necessary to validate the prediction method when the prediction accuracy is close to the measurement results of commercial turbidimeters.

5. Acknowledgment

6. References

[1] M. Hurst, M. Weber-Shirk, and L. W. Lion, "Influence of Alum Coagulant Dose and Influent Turbidity on Floc Blanket Growth Rate, Steady-State Suspended Solids Concentration, and Turbidity Removal," *J. Environ. Eng.*, vol. 143, no. 2, p. 04016081, 2017, doi: 10.1061/(asce)ee.1943-7870.0001131.

[2] J. L. Lin and A. R. Ika, "Enhanced Coagulation of Low Turbid Water for Drinking Water Treatment: Dosing Approach on Floc Formation and Residuals Minimization," *Environ. Eng. Sci.*, vol. 36, no. 6, pp. 732–738, 2019, doi: 10.1089/ees.2018.0430.

[3] L. Takić, D. Vasović, S. Marković, and Z. Burzić, "The Equation for the Optimum Dosage of Coagulant for Water Treatment Plant," *Teh. Vjesn. - Tech. Gaz.*, vol. 26, no. 2, pp. 571–575, 2019, doi: 10.17559/tv-20180213104907.

[4] Q. H. Malik, "Performance of alum and assorted coagulants in turbidity removal of muddy water," *Appl. Water Sci.*, vol. 8, no. 1, pp. 1–4, 2018, doi: 10.1007/s13201-018-0662-5.

[5] American Public Health Association (APHA), "Standard Methods for the Examination of Water & Wastewater 21st Edition," *Am. Public Heal. Assoc. Am. Water Work. A ssociation, Water Environ. Fed.*, 1999.

[6] O. Thomas and C. Burgess, *UV-visible spectrophotometry of water and wastewater*. Elsevier, 2017.

[7] C. N. Sawyer, P. L. McCarty, and G. F. Parkin, *Chemistry for Environmental Engineering and Science*, 5th ed. McGraw-Hill Companies, Inc., 2003.

[8] A. F. Bin Omar and M. Z. Bin Matjafri, "Turbidimeter Design and Analysis: A Review on Optical Fiber Sensors for the Measurement of Water Turbidity," *Sensors*, pp. 8311–8335, 2009, doi: 10.3390/s91008311.

[9] M. Metzger *et al.*, "Low-cost GRIN-Lens-based nephelometric turbidity sensing in the range of 0.1–1000 NTU," *Sensors (Switzerland)*, vol. 18, no. 4, pp. 1–9, 2018, doi: 10.3390/s18041115.

[10] G. Wiranto, I. D. P. Hermida, A. Fatah, and Waslaluddin, "Design and realisation of a turbidimeter using TSL250 photodetector and Arduino microcontroller," *IEEE Int. Conf. Semicond. Electron. Proceedings, ICSE*, vol. 2016-Septe, pp. 324–327, 2016, doi: 10.1109/SMELEC.2016.7573657.

[11] C. A. B. Mello, "An Algorithm for Foreground-Background Separation in Low Quality Patrimonial Document Images," in *Progress in Pattern Recognition, Image Analysis and Applications*, 2007, pp. 911–920.

[12] L. Nichele, V. Persichetti, M. Lucidi, and G. Cincotti, "Quantitative evaluation of ImageJ thresholding algorithms for microbial cell counting," *OSA Contin.*, vol. 3, no. 6, p. 1417, 2020, doi: 10.1364/osac.393971.

[13] P. Choudhry, "High-Throughput method for automated colony and cell counting by digital image analysis based on edge detection," *PLoS One*, vol. 11, no. 2, pp. 1–23, 2016, doi:

10.1371/journal.pone.0148469.

[14]   M. Bosch, "Introduction to ImageJ Macro Language in a Particle Counting Analysis: Automation Matters," in *Computer Optimized Microscopy: Methods and Protocols*, E. Rebollo and M. Bosch, Eds. New York, NY: Springer New York, 2019, pp. 51–70.

[15]   J. Lojk, U. Čibej, D. Karlaš, L. Šajn, and M. Pavlin, "Comparison of two automatic cell-counting solutions for fluorescent microscopic images," *J. Microsc.*, vol. 260, no. 1, pp. 107–116, 2015, doi: 10.1111/jmi.12272.

[16]   I. V. Grishagin, "Automatic cell counting with ImageJ," *Anal. Biochem.*, vol. 473, no. December, pp. 63–65, 2015, doi: 10.1016/j.ab.2014.12.007.

[17]   T. Ferreira and W. Rasband, "ImageJ User Guide User Guide ImageJ," *Image J user Guide*, vol. 1.46r. 2012, doi: 10.1038/nmeth.2019.

[18]   G. P. Freitag, L. G. F. de Lima, L. E. Kozicki, L. C. S. Felicio, and R. R. Weiss, "Use of a smartphone camera attached to a light microscope to determine equine sperm concentration in imagej software," *Arch. Vet. Sci.*, vol. 25, no. 3, pp. 33–45, 2020, doi: 10.5380/avs.v25i3.71839.

[19]   Y. Mulyana and D. L. Hakim, "Prototype of Water Turbidity Monitoring System," *IOP Conf. Ser. Mater. Sci. Eng.*, vol. 384, no. 1, pp. 0–6, 2018, doi: 10.1088/1757-899X/384/1/012052.

[20]   M. Gulyás, N. Bencsik, S. Pusztai, H. Liliom, and K. Schlett, "AnimalTracker: An ImageJ-Based Tracking API to Create a Customized Behaviour Analyser Program," *Neuroinformatics*, vol. 14, no. 4, pp. 479–481, 2016, doi: 10.1007/s12021-016-9303-z.

[21]   C. E. Boyd, "Suspended Solids, Color, Turbidity, and Light," in *Water Quality: An Introduction*, Cham: Springer International Publishing, 2020, pp. 119–133.

[22]   R. C. Peterson and J. S. Wolffsohn, "The effect of digital image resolution and compression on anterior eye imaging," *Br. J. Ophthalmol.*, vol. 89, no. 7, pp. 828–830, 2005, doi: 10.1136/bjo.2004.062240.

[23]   Z. Fu, Y. Chen, H. Yong, R. Jiang, L. Zhang, and X. S. Hua, "Foreground Gating and Background Refining Network for Surveillance Object Detection," *IEEE Trans. Image Process.*, vol. 28, no. 12, pp. 6077–6090, 2019, doi: 10.1109/TIP.2019.2922095.